Low-Profile Asymmetrical-CSRR-Loaded Stacked Microstrip Patch Antenna

Ming-Chun Tang[1], Ting Shi[1], Han Xiong[1], and Shaowei Qing[2]

[1]College of Communication Engineering, Chongqing University, Chongqing 400044, China
tangmingchunuestc@126.com, shiting100220@gmail.com, xiong1226han@126.com

[2]Power Engineering Institute, Chongqing University, Chongqing 400044, China
qshaowei@gmail.com

Abstract **–** By introducing an asymmetrical-CSRR-loaded parasitic patch beneath the radiating patch of a traditional low-profile microstrip antenna, a novel stacked antenna with both 22.46% fractional bandwidth, and stable and uniform radiation patterns in the entire operating frequency range is achieved, even the total height is only approximate $0.04\lambda_L$ (where λ_L indicates the free-space wavelength corresponding to the lower bound of the operating frequency band). The antenna is designed, fabricated and tested. The experimental results agree with the simulations.

Index Terms **–** Low-profile antenna, microstrip patch antenna, wideband.

I. INTRODUCTION

Low-profile microstrip patch antenna is one of the most commonly used antenna types, due to its excellent performance characteristics, including robust design, low cost, easy integration with other microwave devices, and so on. However, one typical low-profile microstrip patch antenna in the basic form of a rectangle- or circular-shaped conducting radiating patch in a grounded substrate is inherently narrowband and is thus not able to meet the requirements of most wireless communication systems nowadays [1-3]. In order to increase the operational bandwidth, a lot of effective approaches arise to the date [4]. As one of the popular technologies, parasitic patches were applied to place on the second layer of patch antennas to design new stacked antennas. This resort could create another resonance in conjunction with the main resonance, which exploring wide overall operational bandwidth. On one hand, by employing a parasitic patch on the second layer with identical configuration and with the electrical size close to the main radiating patch, a wider operational frequency range, which is contributed by two adjacent resonances, i.e., radiating patch resonance and parasitic patch inherent resonance, was accomplished [5]. On the other hand, with the usage of a slotted parasitic patch on the second layer, the distributed LC circuit originating from the slot introduces a second resonance, which could combine the main patch resonance to widen the impedance bandwidth [6]. While effective, these approaches witness a drawback that the addition of one layer could produce only one resonance to do good to bandwidth increase. Logically, one can anticipate that, while maintaining the antenna's low profile, more resonances or wider bandwidth could be explored by only applying more layers based on above stacked antenna design technologies, which would significantly increase the complexity in design and fabrication process. In this letter, by introducing only one asymmetrical-CSRR-slotted parasitic patch on the second layer in a typical low-profile microstrip antenna design, two other adjacent resonances are obtained simultaneously to gain much wider operating frequency range.

II. ANTENNA DESIGN AND CONFIGURATION

The antenna configurations are presented in Fig. 1. The antenna is constructed by two pieces of 0.018-mm-thick copper, 1.6 mm FR4 substrate (ε_r=4.4, μ_r=1.0, loss tangent = 0.02) in sandwich stacking arrangement. And two sheets are connected with two pairs of long hexagonal plastic nuts and screws. In simulation, they are modeled as vias/posts that pass slightly through the substrates of both sheets, which are depicted in Fig. 1 (a). As shown in Figs. 1 (b) and (c), a radiating patch with modified configuration is designed on layer 1, which has one rectangle slot ($L_4\times W_5$) and one rectangle strip ($L_3\times W_3$). The rectangle slot is designed to make more EM energy leaking from the complementary split ring resonator (CSRR) slot resonance, in order to make high overall efficiency from the slot resonance. The rectangle strip on the other side of radiating patch is to provide more tuning freedoms to accommodate the degradation of impedance match characteristics due to the presence of the slotted parasitic patch, instead of only tuning the

Submitted On: December 4, 2014
Accepted On: June 11, 2015

position of feed probe along the *x*-axis. In Fig. 1 (d), a slotted parasitic patch is designed with the length L_7 on layer 2, which is determined a little lower than the radiating patch (L_2+L_3). It could provide a little higher and overlapping resonance frequency band to aid the impedance bandwidth improvement. In order to avoid shorting with the feeding probe (with the radius R_4), a larger hole (with the radius R_3) on the parasitic patch is constructed. Note that, the hole is a little offset from the centre of parasitic patch. The offset could tune the parasitic patch operating in good impedance match performances. Moreover, a CSRR structure with asymmetrical configuration, serving as an additional near-field-resonant-parasitic (NFRP) element [7,8], is placed offset from the centre of parasitic element (L_{10}-L_9).

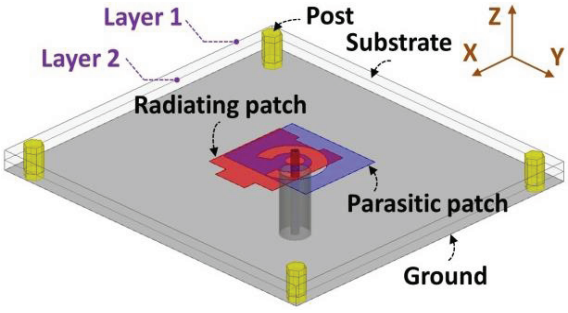

(a)

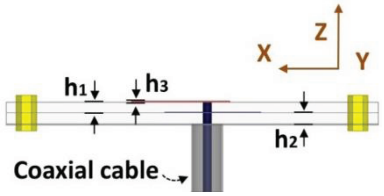

(b)

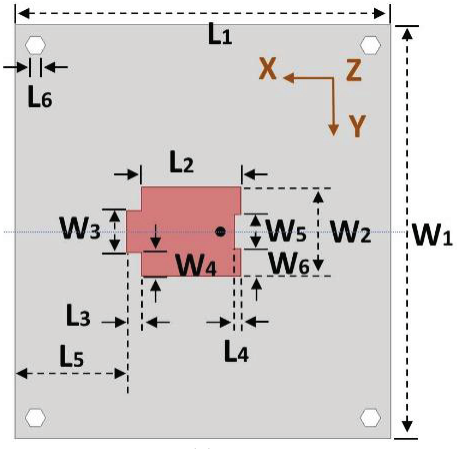

(c)

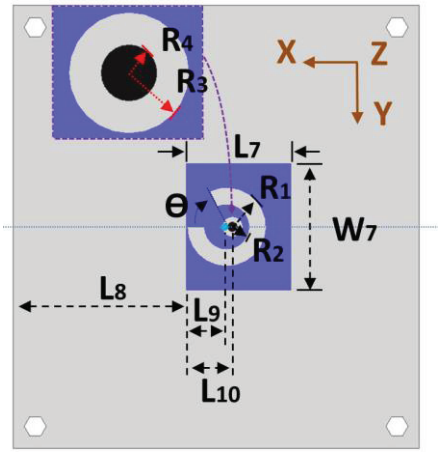

(d)

Fig. 1. Patch antenna: (a) 3D isometric view, (b) side view, (c) top view of layer 1, and (d) top view of layer 2.

It is worth pointing out that, the reason for designing the CSRR with such asymmetrical configuration is that, while maintaining the fundamental resonance frequency (which is corresponding to the total electrical length) of CSRR structure close enough to the two resonances from the patches, the surface current around the slot structure could be well induced to create a considerably wide operating band to be overlapping with the other two operating bands, thus widen the entire operating frequency range. The determined geometry parameters are as follows (in millimeters): h_1=1.6, h_2=1.6, h_3=0.018, L_1=55, L_2=14.55, L_3=2.2, L_4=1, L_5=16.35, L_6=1.5, L_7=14.2, L_8=23.45, L_9=5.475, L_{10}=6.275, W_1=60, W_2=13, W_3=6, W_4=3.5, W_5=5, W_6=4, W_7=17, R_1=5.35, R_2=3, R_3=1.4, and R_4=0.65. And the arc-shaped gap radian of the CSRR is $\theta = 0.36\pi$. We note that, according to our simulation investigation, tuning θ could not only change the resonance frequency centre of CSRR, but also shift the impedance characteristics in the entire operating band.

III. EXPERIMENTAL RESULTS AND DISCUSSION

The NFRP-based patch antenna shown in Fig. 1 was fabricated and its performance characteristics were obtained experimentally. The reflection coefficient of the antenna was measured using an Agilent E8361A PNA Vector Network Analyzer (VNA). The simulated and measured $|S_{11}|$ values together with the fabricated prototype are depicted in Fig. 2. As anticipated from the frequency domain ANSYS/ANSOFT High Frequency

Structure Simulator (HFSS) simulations, the antenna operates from 4.115 GHz to 5.045 GHz (20.31% fractional bandwidth), with three resonance dips located at 4.230 GHz, 4.555 GHz and 4.955 GHz, respectively. The measured results show that, it operates from 4.15 GHz to 5.20 GHz (22.46% fractional bandwidth), with three resonance dips located at 4.25 GHz, 4.655 GHz, and 5.12 GHz, respectively. Accordingly, the antenna total height ($h_1+h_2+2\times h_3$), evaluated at the lower frequency bound f_L=4.15GHz, is 0.044λ_L, where λ_L is the free-space wavelength corresponding to the lower frequency bound (λ_L=c/f_L). Obviously, the measured results, together with the full-wave simulations, show expected wide impedance bandwidth with three resonance modes, which are mainly from the radiating and parasitic patches' inherent resonances and the sub-wavelength resonance from CSRR slot, respectively. A little lack of agreement between the operating bandwidths of the simulated and measured designs may be due to an air gap between the two substrate layers which is absent in simulations, and some other minor errors in the fabrication, installation, and experimental process [9]. Moreover, acting as the reference antenna, one antenna without parasitic patch is designed and its impedance match is shifted to optimum (by only moving the radiating patch position (L_5) from 15.35 mm to 18.35 mm along *x*-axis). The refection coefficient is also presented in Fig. 2 for comparison. Clearly, it could operate in the centre of 4.14 GHz with $|S_{11}|_{min}$ < -20 dB and bandwidth from 4.05 GHz to 4.24 GHz (only 4.58% fractional bandwidth), as was expected [4]. Therefore, it could be readily concluded from the comparison that, the addition of the parasitic patch provides a little higher (only 2.5% blue shift of the lower frequency bound) but much wider impedance bandwidth (approximately 5 times fractional bandwidth achievement).

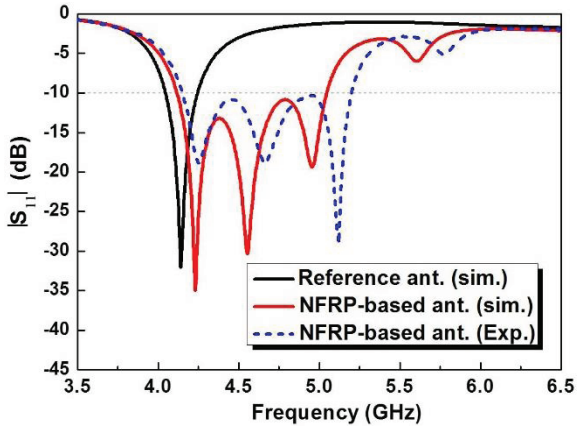

(a)

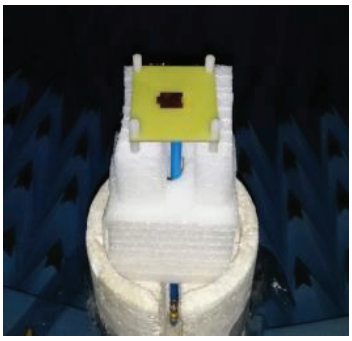
(b)

Fig. 2. Simulated and measured input impedance characteristics of two low-profile patch antennas: (a) reflection coefficients ($|S_{11}|$ values in dB), and (b) the fabricated phototype in the chamber.

The far-field realized gain patterns were measured in an anechoic chamber. The chamber is based mainly on the Agilent EB362C PNA VNA and the SATIMO passive measurement system. The corresponding simulated and measured *E*- and *H*-plane total realized gain patterns at three selected frequency points within the operational bandwidth are shown in Fig. 3. In details, the measured (simulated) peak realized gains are 4.96 dB (5.0045 dB), 5.55 dB (4.9520 dB), and 2.61 dB (3.0523 dB) at 4.25 GHz (4.23 GHz), 4.66 GHz (4.555 GHz), and 5.12 GHz (4.955 GHz), respectively. It is clear in Fig. 3 that, almost uniform radiation patterns and around 3 dB peak realized total gain variations in both the simulation and experimental results indicate its relatively stable radiation performance characteristics. In addition, as is observed in Fig. 3 (c), only a little asymmetry of main radiation beam appears in the higher frequency range. This phenomenon is ascribed to the asymmetrical CSRR structure.

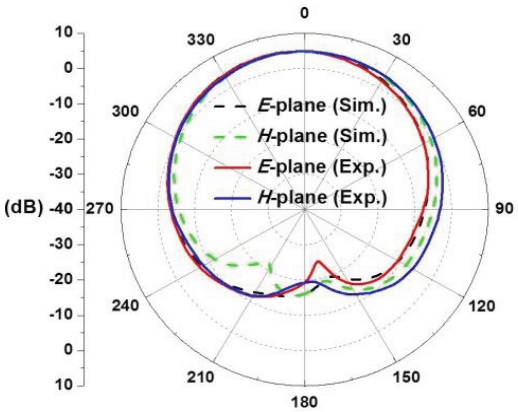

(a)

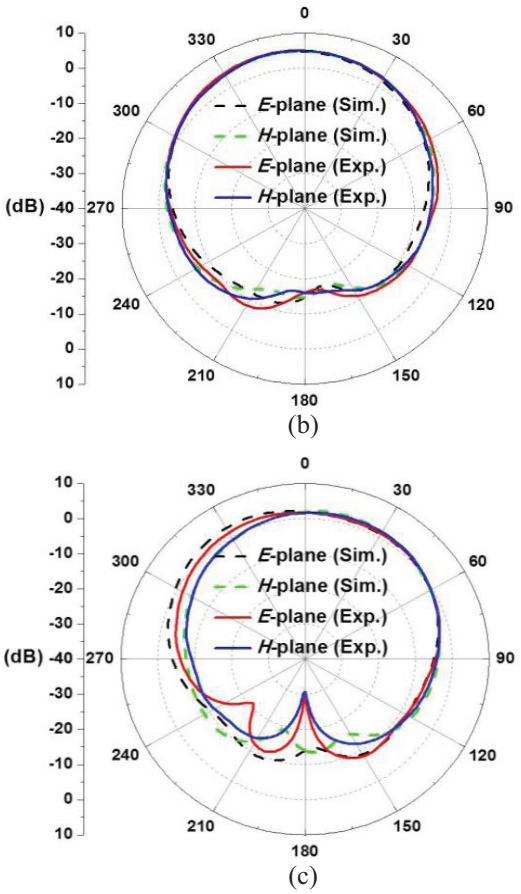

Fig. 3. Simulated and measured total realized gain patterns in the *E*- and *H*-planes at three frequency points: (a) 4.230 GHz in simulation and 4.25 GHz in measurement, (b) 4.555 GHz in simulation and 4.66 GHz in measurement, and (c) 4.955 GHz in simulation and 5.12 GHz in measurement.

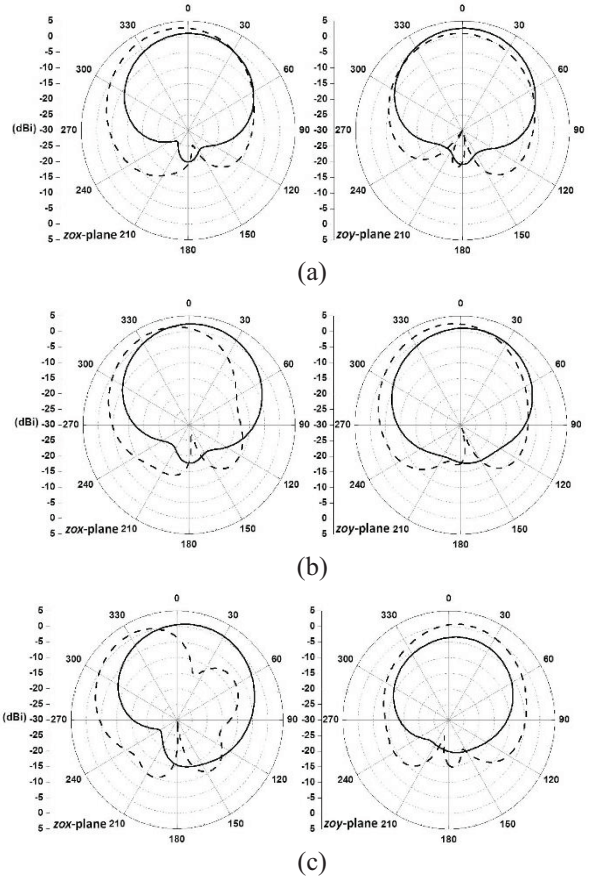

Fig. 4. Simulated realized gain patterns in the *E*- and *H*-planes at three frequency points: (a) at 4.230 GHz, (b) at 4.555 GHz, and (c) at 4.955 GHz. Here, *E*-phi and *E*-theta are indicated in solid and dashed lines, respectively.

To further study its radiation characteristics in the entire frequency band, more simulated results are presented in Figs. 4-5. Figure 4 gives its corresponding realized gain patterns in *zox* (*E*)-plane and *zoy* (*H*)-plane at the three resonance frequency centers. According to the radiation patterns, it is obvious that the cross-polarization is significantly higher than the traditional patch antenna. This characteristic could make the proposed antenna be advantageous for some special applications, such as the indoor wireless communication since it would lead to better transmission capability in rich multipath environment [10-11]. On the other hand, as is shown in Fig. 5, in such a wide operational frequency range, the peak realized gain value fluctuates in the range from 2.56 dBi to 5.25 dBi (2.69 dB variation), and the radiation efficiency is varied from 45.1% to 67.9% (22.8% fluctuation).

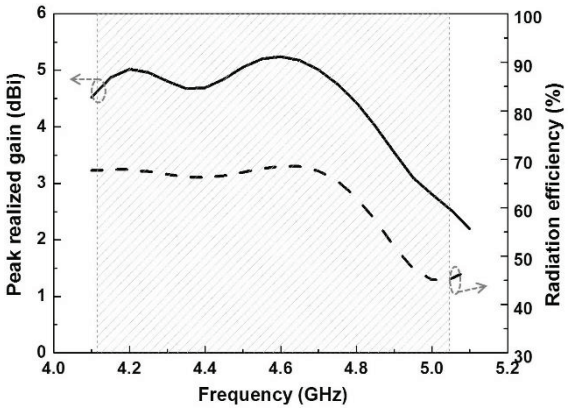

Fig. 5. Simulated peak realized gain and radiation efficiency values as a function of frequency.

IV. CONCLUSION

A NFRP-based, low-profile, wideband stacked

microstrip patch antenna is introduced in this letter. By introducing an asymmetrical-CSRR-loaded parasitic patch on the second layer beneath the radiating patch of a traditional microstrip antenna, a much wider bandwidth (approximate 5 time achievement), and relatively stable and uniform radiation patterns in the entire operating frequency range, are both obtained. Measured performance agrees well with simulation. The performance is very advantageous for wideband and low-cost stacked microstrip patch antenna designs on future mobile terminals.

ACKNOWLEDGMENT

This work was supported in part by the National Natural Science Foundation of China contract number 61471072, and in part by the Fundamental Research Funds for the Central Universities contract numbers 106112015CDJZR165510 and 106112015CDJXY160007.

REFERENCES

[1] M.-C. Tang, S. Xiao, D. Wang, C. Wei, and B. Wang, "A compact planar negative permittivity ZOR antenna," *J. of Electromagn. Waves and Appl.*, vol. 25, pp. 1122-1130, 2011.

[2] J. Xiong, X. Lin, Y. Yu, M.-C. Tang, S. Xiao, and B. Wang, "Novel flexible dual-frequency broadside radiating rectangular patch antennas based on complementary planar ENZ or MNZ metamaterials," *IEEE Trans. Antennas Propag.*, vol. 60, no. 8, pp. 3958-3961, Aug. 2012.

[3] M.-C. Tang, S. Xiao, T. Deng, H. Zhu, and B.-Z. Wang, "Design of compact, low-profile, wideband, dual-frequency patch antennas based on complementary co-directional SRRs," *IEEE Antennas Propag. Mag.*, vol. 56, no. 6, pp. 72-89, Dec. 2014.

[4] K.-F. Lee and K.-F. Tong, "Microstrip patch antennas - basic characteristics and some recent advances," *Proc. IEEE*, vol. 100, pp. 2169-2180, 2012.

[5] L. Barlatey, J. R. Mosig, and T. Sphieopoulos, "Analysis of stacked microstrip patches with a mixed potential integral equation," *IEEE Trans. Antennas Propag.*, vol. 38, pp. 608-615, 1990.

[6] Y. Chen, S. Yang, and Z. Nie, "Bandwidth enhancement method for low profile E-shaped microstrip patch antennas," *IEEE Trans. Antennas Propag.*, vol. 58, pp. 2442-2447, 2010.

[7] M.-C. Tang and R. W. Ziolkowski, "Efficient, high directivity, large front-to-back-ratio, electrically small, near-field-resonant-parasitic antenna," *IEEE Access*, vol. 1, pp. 16-28, 2013.

[8] M.-C. Tang, R. W. Ziolkowski, S. Xiao, and M. Li, "A high-directivity, wideband, efficient, electrically small antenna system," *IEEE Trans. Antennas Propag.*, vol. 62, pp. 6541-6547, 2014.

[9] A. Buerkle, K. Sarabandi, and H. Mosallaei, "Compact slot and dielectric resonator antenna with dual-resonance, broadband characteristics," *IEEE Trans. Antennas Propag.*, vol. 53, pp. 1020-1027, 2005.

[10] K.-L Wong, *Compact and Broadband Microstrip Antennas*, New York: Wiley, ch. 3, 2002.

[11] J.-Y. Pang, S.-Q. Xiao, S.-T. Chen, and B.-Z. Wang, "Compact and wideband PIFA for DCS/PCS/UMTS/WLAN communication system," *Microw. Opt. Technol. Lett.*, vol. 52, pp. 1097-1100, May 2010.